Temperature-independent silicon subwavelength grating waveguides

Schmid, J. H.; Ibrahim, M.; Cheben, P.; Lapointe, J.; Janz, S.; Bock, P. J.; Densmore, A.; Lamontagne, B.; Ma, R.; Ye, W. N.; Xu, D.-X.

Publisher's version / Version de l'éditeur:
https://doi.org/10.1364/OL.36.002110
Optics Letters, 36, 11, pp. 2110-2112, 2011-06-01

Temperature-independent silicon subwavelength grating waveguides

J. H. Schmid,[1,*] M. Ibrahim,[2] P. Cheben,[1] J. Lapointe,[1] S. Janz,[1] P. J. Bock,[1] A. Densmore,[1] B. Lamontagne,[1] R. Ma,[1] W. N. Ye,[2] and D.-X. Xu[1]

[1]*Institute for Microstructural Sciences, National Research Council Canada, Ottawa, Ontario K1A 0R6, Canada*

[2]*Department of Electronics, Carleton University, Ottawa, Ontario K1S 5B6, Canada*

**Corresponding author: jens.schmid@nrc-cnrc.gc.ca*

Received April 4, 2011; accepted April 14, 2011;
posted April 21, 2011 (Doc. ID 145382); published May 31, 2011

We demonstrate, by experiment and numerical calculations, temperature-independent subwavelength grating waveguides with a periodic composite core composed of alternating regions of silicon and SU-8 polymer. The polymer has a negative thermo-optic (TO) material coefficient that cancels the large positive TO effect of the silicon. Measurements and Bloch mode calculations were carried out over a range of silicon–polymer duty ratios. The lowest measured TO coefficient at a wavelength of 1550 nm is $1.8 \times 10^{-6}\,\mathrm{K}^{-1}$; 2 orders of magnitude smaller than a conventional silicon photonic wire waveguide. Calculations predict the possibility of complete cancellation of the silicon waveguide temperature dependence.

OCIS codes: 130.3120, 050.6624, 130.3130.

In recent years, much progress has been reported in the development of integrated silicon photonic devices and circuits, which are expected to have a major impact on optical interconnects and data transport applications. High index contrast silicon microphotonic waveguides are also used in emerging new applications in biosensing [1] and spectroscopy [2]. An important issue with silicon photonic circuits is the temperature dependence of their optical output signals, which is caused by the comparatively high thermo-optic (TO) material coefficient of silicon ($dn_{Si}/dT = 1.8 \times 10^{-4}\,\mathrm{K}^{-1}$). Precise external temperature control is, therefore, often required for silicon photonic devices, especially those incorporating interferometers, resonators, and wavelength dispersive elements. The temperature dependence of silicon wire waveguides can be reduced by using a polymer overcladding with a negative TO coefficient to compensate for the silicon TO effect [3,4]. Athermal operation of waveguides, i.e., $dn_{\mathrm{eff}}/dT = 0$, where n_{eff} is the mode effective index and T is the ambient temperature, is achieved if waveguide dimensions are chosen such that the relative overlap of the mode with the silicon core and the polymer cladding results in a cancellation of their respective contributions to the waveguide effective TO coefficient. This can be accomplished in narrow silicon wires with a fairly delocalized mode [5], or with slot waveguides, in which a large fraction of the modal field is confined to a narrow gap filled with the low-index polymer [6].

Here we suggest a new principle for making athermal silicon waveguides, using the subwavelength grating (SWG) effect. We have recently demonstrated that silicon photonic wire waveguides with periodic gaps, of a period smaller than one-half of the effective operating wavelength, act as low-loss waveguides with a spatially averaged core index [7]. A schematic illustration of a SWG waveguide is shown in Fig. 1(a). In short, SWG waveguides operate in the long wavelength regime of the dispersion diagram, well below the frequency of the first stop band. Their fundamental mode is a bound Bloch mode, which is, in principle, lossless. Since the period of the grating etched into the waveguide is well below the operating wavelength, its fine structure is not resolved by the light and diffraction is suppressed. Therefore, the optical properties of the SWG waveguide resemble those of a channel waveguide with a spatially averaged core index. Spatial index averaging offers the opportunity of mitigating the silicon TO effect by filling the gaps with polymer material of negative TO coefficient for an appropriate grating duty ratio. The polymer used in our work is SU-8, which has a refractive index of $n_{\mathrm{SU\text{-}8}} \sim 1.58$ at $\lambda = 1.55\,\mu\mathrm{m}$ and a TO coefficient of $dn_{\mathrm{SU\text{-}8}}/dT = -1.1 \times 10^{-4}\,\mathrm{K}^{-1}$ [8].

In Figs. 1(b)–1(d), we show scanning electron microscope images of three fabricated SWG waveguides of 470 nm width, 250 nm grating pitch, and duty cycles of (b) 46%, (c) 56%, and (d) 66%. These waveguides were fabricated from commercial silicon-on-insulator substrates with $0.26\,\mu\mathrm{m}$ thick silicon and $2\,\mu\mathrm{m}$ thick buried oxide layers. We used electron beam lithography to define the waveguides and transferred the pattern into the silicon layer by inductively coupled plasma reactive ion etching using a mixture of SF_6 and C_4F_8 gases. The samples were coated with a 2-μm-thick SU-8 polymer layer by a standard spin and bake procedure. To measure the TO coefficient of the composite silicon–polymer SWG waveguides, the structures were incorporated in unbalanced Mach–Zehnder interferometer (MZI) devices, as shown in Fig. 1(d). Standard photonic wire waveguides are used for the Y splitters, and the waveguide bends while each arm of the MZI includes two straight SWG sections. Wire waveguides are adiabatically transformed to SWG waveguides at the positions indicated by arrows in Fig. 1(e), with coupler structures similar to the one described in [9]. The combination of wire and SWG waveguides in the same device demonstrates the compatibility of the two waveguide types. SWG waveguide propagation loss has previously been found to be of comparable magnitude to our photonic wires [7]. The two arms of the MZI are identical except for the additional SWG section length of $\Delta L = 3\,\mathrm{mm}$ inserted into the upper arm. The transmitted intensity of the MZI interferometers will, therefore, have the usual sinusoidal form

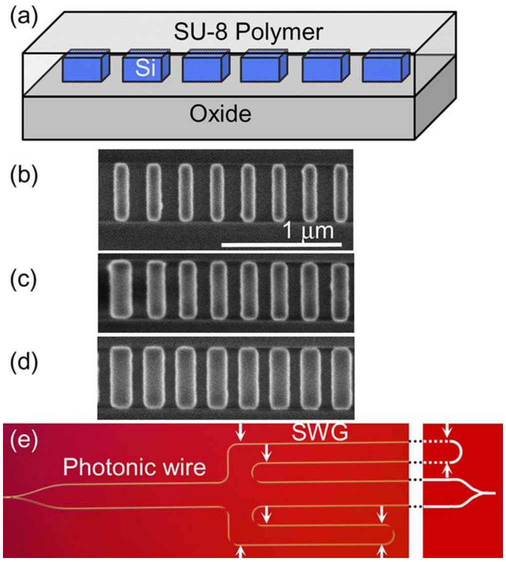

Fig. 1. (Color online) (a) Schematic of an SU-8 clad silicon SWG waveguide. (b)–(d) SEM micrographs of SWG waveguides with duty cycles of 46%, 56%, and 66%. (e) Optical micrograph of an unbalanced MZI device with SWG sections. Arrows indicate the positions of wire-to-SWG waveguide couplers. The continuation of the device beyond the field of view is indicated schematically on the right-hand side of the picture for clarity.

$I = \cos^2(k_0/2\ n_{\text{eff}}\ \Delta L)$, where n_{eff} is the effective index of the silicon–polymer composite SWG section.

Figure 2 shows the results for optical transmission of MZI devices with SWG waveguides of varying duty cycles at different temperatures. For these measurements, the chips were mounted on a temperature-controlled copper heat sink. For waveguides with a duty cycle of 100%,

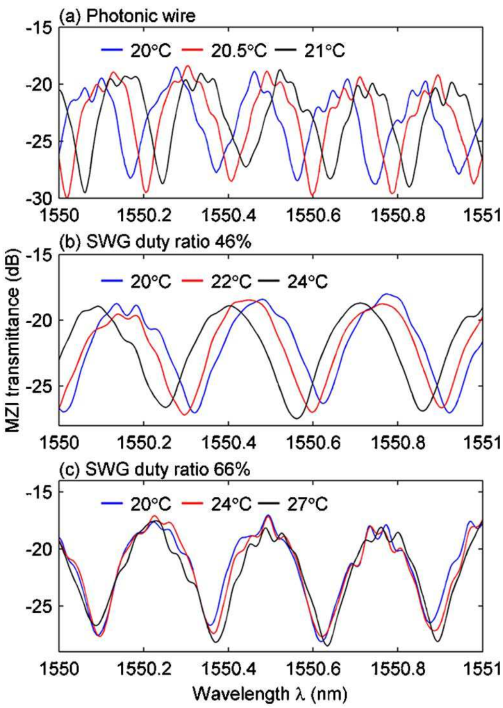

Fig. 2. (Color online) Temperature-dependent transmission spectra of MZI devices for different SWG duty ratios. A sign reversal from negative to positive temperature-induced wavelength shifts is observed for increasing duty cycle.

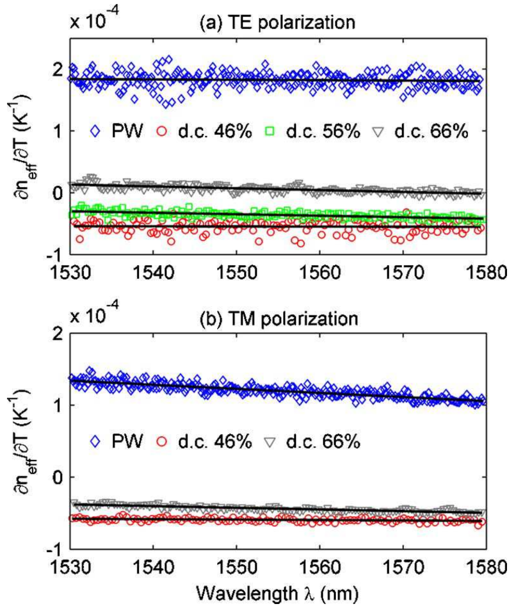

Fig. 3. (Color online) Measured TO coefficient of photonic wire (PW) and SWG waveguides of various duty cycles (d.c.) indicated in the figure as functions of wavelength with linear fits (solid lines). (a) TE and (b) TM polarization.

i.e., conventional photonic wire waveguides, a positive wavelength shift of approximately 70 pm/°C is observed [Fig. 2(a)]. In comparison, the sign of the shift is reversed and the magnitude reduced for SWG waveguides with a duty cycle of 46%, as seen in Fig. 2(b). For the SWG waveguides with a duty cycle of 66% in Fig. 2(c), the temperature-dependent shift of the transmission spectrum is minimal, indicating nearly athermal waveguide behavior. All spectra shown in Fig. 2 are for quasi-TE polarization.

For our configuration of the MZI device, the waveguide TO coefficient dn_{eff}/dT can be derived from the wavelength shift $d\lambda/dT$ of the transmission spectra:

$$\frac{dn_{\text{eff}}}{dT} = \frac{n_g}{\lambda}\frac{d\lambda}{dT}, \tag{1}$$

where n_g is the group index of the waveguide, which is related to the period $\Delta\lambda$ of the MZI transmission by $n_g = \lambda^2/(\Delta\lambda\Delta L)$. We calculated the TO coefficient as a function of wavelength from the observed temperature-induced spectral shifts of the transmission minima. The results are plotted in Fig. 3 over a 50 nm spectral range, where each data point corresponds to the measured shift of one transmission minimum. Solid lines are linear fits to the data. For TE polarization [Fig. 3(a)], the TO coefficients of SWG waveguides with duty ratios of 46% and 56% are negative, while the TO coefficient of the photonic wire is positive, as expected. For a 66% duty ratio, the SWG waveguide is nearly athermal, consistent with the small wavelength shifts observed in Fig. 2(c). For this waveguide, the coefficients of the linear fit function $f = a\lambda + b$ are given by $a = -2.95 \times 10^{-7}\ \text{nm}^{-1}\ \text{K}^{-1}$ and $b = 4.65 \times 10^{-4}\ \text{K}^{-1}$, which yields athermal operation for a wavelength of 1576 nm. For TM polarization [Fig. 3(b)], a positive TO coefficient is measured for the photonic wire device, whereas the coefficient is negative for the segmented SWG waveguides with these

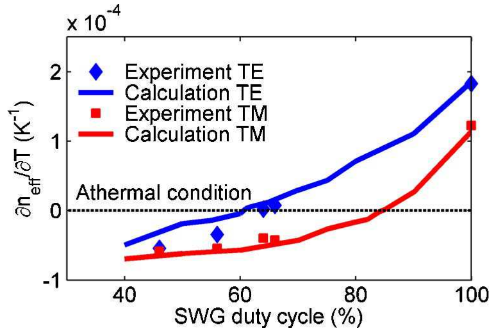

Fig. 4. (Color online) Experimental and theoretical results for the effective TO coefficient of SU-8 clad silicon SWG waveguides as a function of grating duty cycle.

duty cycles. While none of the measured SWG waveguides exhibits athermal behavior for TM polarization, it is obvious from the observed sign reversal of the TO coefficient that athermal TM operation exists for a duty ratio between 66% and 100%.

The values of the linear fits shown in Fig. 3 for the TO coefficient dn_{eff}/dT at the wavelength $\lambda = 1550\,\mathrm{nm}$ are plotted as functions of SWG duty ratio in Fig. 4 for both TE and TM polarizations (blue diamonds and red squares). Our full data set plotted in Fig. 4 also includes a waveguide with duty ratio of 64%, which, for clarity, is not shown in Fig. 3. The experiment confirms the expected decrease of the TO coefficient with decreasing duty ratio, including sign reversal and near athermal behavior for TE waveguides with a duty cycle of approximately 65%. At $\lambda = 1550\,\mathrm{nm}$, our lowest measured value for the TO coefficient is $1.8 \times 10^{-6}\,\mathrm{K}^{-1}$ for a duty ratio of 64%. The experimental data is compared to calculations with the MIT photonic bands software [10], which is used as a mode solver for the periodic waveguides. To find the TO coefficient numerically, we first calculate the dispersion (ω–k) diagram of the SWG waveguide using the room-temperature values of the material refractive indices ($n_{\mathrm{Si}} = 3.476$, $n_{\mathrm{SU8}} = 1.58$ and $n_{\mathrm{SiO_2}} = 1.444$). The waveguide effective index at $\lambda = 1.55\,\mu\mathrm{m}$ is obtained directly from the calculated dispersion, $n_{\mathrm{eff}} = ck/\omega$, where c is the speed of light. The calculation is then repeated for the same structure at a different temperature. The refractive indices of the constituent materials are changed from their room-temperature values to reflect a temperature increase of 20 K according to their respective TO coefficients. From the results of the two calculations, the derivative dn_{eff}/dT is determined. We overlaid the results of this calculation with the experimental data in Fig. 4. For the photonic wire waveguide, we obtain $dn_{\mathrm{eff}}/dT = 1.8 \times 10^{-4}\,\mathrm{K}^{-1}$ and $1.2 \times 10^{-4}\,\mathrm{K}^{-1}$ for TE and TM polarization, respectively, in good agreement with the measured values. As the duty ratio of the SWG waveguides is lowered by increasing the gap size, we observe a transition from positive to negative TO coefficients for both polarizations, as is also observed in the experiment. The zero crossing, corresponding to an athermal waveguide, occurs for a duty ratio of 61% for TE and 85% for TM. The higher duty ratio required for athermal operation for TM polarization is due to the fact that the electromagnetic boundary conditions cause the TM mode of our thin SWG waveguide to be more delocalized vertically than the TE mode, leading to a larger overlap with the SU-8 cladding above the waveguide for all duty ratios. To compensate for this effect, the volume ratio of the silicon material inside the composite waveguide core needs to be increased accordingly. Overall, the match of experimental data and numerical calculations is excellent and validates our strategy of mitigating the TO effect in optical waveguides by subwavelength patterning.

In conclusion, we have demonstrated that the subwavelength grating spatial averaging effect can be used to make temperature-independent waveguides with a composite core consisting of silicon and SU-8 polymer, compatible with standard silicon photonic wire waveguides. Athermal behavior can be achieved for both TE and TM polarization, albeit for different SWG duty ratios. These results on engineering the TO waveguide properties using subwavelength gratings are thought to be a significant step forward toward developing temperature-insensitive silicon photonic circuits.

References

1. A. Densmore, D.-X. Xu, P. Waldron, S. Janz, P. Cheben, J. Lapointe, A. Delâge, B. Lamontagne, J. H. Schmid, and E. Post, IEEE Photon. Technol. Lett. **18**, 2520 (2006).
2. P. Cheben, J. H. Schmid, A. Delâge, A. Densmore, S. Janz, B. Lamontagne, J. Lapointe, E. Post, P. Waldron, and D.-X. Xu, Opt. Express **15**, 2299 (2007).
3. J.-M. Lee, D.-J. Kim, H. Ahn, S.-H. Park, and G. Kim, J. Lightwave Technol. **25**, 2236 (2007).
4. W. N. Ye, J. Michel, and L. C. Kimerling, IEEE Photon. Technol. Lett. **20**, 885 (2008).
5. J. Teng, P. Dumon, W. Bogaerts, H. Zhang, X. Jian, X. Han, M. Zhao, G. Morthier, and R. Baets, Opt. Express **17**, 14627 (2009).
6. J.-M. Lee, D.-J. Kim, G.-H. Kim, O-K. Kwon, K.-J. Kim, and G. Kim, Opt. Express **16**, 1645 (2008).
7. P. J. Bock, P. Cheben, J. H. Schmid, J. Lapointe, A. Delâge, S. Janz, G. C. Aers, D.-X. Xu, A. Densmore, and T. J. Hall, Opt. Express **18**, 20251 (2010).
8. P. Rabiei, W. H. Steier, C. Zhang, and L. R. Dalton, J. Lightwave Technol. **20**, 1968 (2002).
9. P. Cheben, P. J. Bock, J. H. Schmid, J. Lapointe, S. Janz, D.-X. Xu, A. Densmore, A. Delâge, B. Lamontagne, and T. J. Hall, Opt. Lett. **35**, 2526 (2010).
10. http://ab-initio.mit.edu/wiki/index.php/MIT_Photonic_Bands.